ELSEVIER

Chemical Engineering Journal 79 (2000) 103–111

Chemical Engineering Journal

www.elsevier.com/locate/cej

Characterization of hydrodynamic dispersion in a chromatographic column under compression

Karin C.E. Östergren*, Christian Trägårdh

Department of Food Engineerig, Lund University, PO Box 124, S-221 00 Lund, Sweden

Received 4 March 1999; received in revised form 28 February 2000; accepted 1 March 2000

Abstract

The efficiency of a compressible, packed chromatographic bed has been characterized experimentally and by computer simulations. The experimental measurements were performed in situ by monitoring the propagation of a tracer using three sets of concentrically located electrodes. The results obtained were compared with results obtained for the same column packed with rigid, non-porous glass beads. Both columns featured a core, characterized by a flat velocity profile and a nearly constant hydrodynamic dispersion. The velocity variations, as well as hydrodynamic dispersion anomalies, in the wall region were found to be smaller in the compressed bed than in the column packed with rigid glass beads. The hydrodynamic dispersion in the compressed column was found to be approximately twice that expected for a column packed with rigid particles under the same conditions. The computed velocity variations in the compressible bed were found to agree qualitatively with experimental data.

Keywords: Chromatography; Dispersion; Compression; Column efficiency; Flow field

1. Introduction

The optimal use of chromatography is especially important in preparative chromatography, where the economy of the process must always be taken into account [1]. Expensive and time-consuming experimental work could be minimized if a numerical model could be used to predict the performance of a chromatographic column. The development of such a model requires a fundamental understanding of both the physical and chemical processes taking place in the column.

To achieve high column efficiency, it is important that the flow characteristics are, as nearly as possible, the same as those of plug flow. Structural variations across the chromatographic bed will cause flow anomalies and decrease the efficiency of the chromatographic process [1–8]. In a compressed column, not only will the velocity profile contribute to the overall hydrodynamic dispersion, but also the local hydrodynamic dispersion itself may also change due to the different packing structures [9].

To predict the velocity field and the hydrodynamic dispersion in a chromatographic column, the factors influencing the structure must be clearly identified and understood. Much effort has been devoted to characterize flow and dispersion in rigid chromatographic beds [2–8,10–14] and most investigations have been performed in narrow columns. This work, however, is focused on the hydrodynamics in process-size columns containing a compressible chromatographic packing.

In previous studies, the compression of a non-rigid chromatographic bed during flow has been investigated, and a two-dimensional model, which predicts the structural changes in the bed due to compression and the corresponding velocity field, assuming a pure elastic deformation, has been proposed [15,16]. In the present study, the efficiency of a chromatographic column with an inner diameter of 0.113 m was investigated. The influence of the compression on the axial, hydrodynamic dispersion coefficient and the velocity profile was experimentally investigated in situ using concentric electrodes imbedded in the chromatographic bed. The experimental results were compared with those obtained for a column packed with glass beads and with theoretical predictions using the model developed previously [15,16].

2. Background

2.1. Non-uniformities of flow

Velocity variations in a chromatographic bed may be caused by inhomogeneities in the stationary phase or

* Corresponding author. Fax: +46-46-2224622.
E-mail address: karin.ostergren@livstek.lth.se (K.C.E. Östergren)

1385-8947/00/$ – see front matter
PII: S1385-8947(00)00165-0

viscosity and density variations in the fluid phase [11]. In the work of Yun and Guiochon [4], the impact of velocity variations was theoretically investigated for different, hypothetical, velocity profiles across the column. The ratio of the maximum to minimum velocity was between 1 and 1.10. Significant changes in the elution profiles were found.

Experimental evidence of radial velocity variations caused by inhomogeneities in the bed has been put forward by, among others, Knox et al. [2], Knox and Patcher [5], Farkas et al. [6], Wilhelm et al. [12], Eon [3], Baur et al. [7] and more recently by Mitchell et al. [8], who were able to obtain three-dimensional concentration distributions in a single solute elution using magnetic resonance imaging. Radial inhomogeneities in wide columns packed with a rigid stationary phase may be due to packing instabilities [13]. This type of non-uniformity is not yet predictable [14]. Velocity profiles may arise in narrow columns due to differences in the packing structure close to the wall. Ideally, the wall region is about 10 particle-diameters thick [17]. A wall-region about 30 particle-diameters thick, characterized by high hydrodynamic dispersion, has been identified experimentally in chromatographic columns [2,6].

In columns packed with non-rigid chromatographic media, variations in the void fraction occur [1,18–21]. The compaction in the axial direction arises from the fluid stress. Variations in the radial direction arise from the wall friction, which opposes the compaction/relaxation [15,16,22]. The velocity variations in compressible, packed columns can be predicted by two-dimensional models, taking into account the mechanical properties of the stationary phase as well as the fluid dynamics [15,16].

2.2. Hydrodynamic dispersion

The hydrodynamic dispersion of a tracer is the result of convection and molecular diffusion. Convective dispersion results from the tortuous path through the porous medium and the mixing of streamlines with different concentrations due to the velocity profile in the individual pores. The effect of the molecular diffusion is also twofold; firstly there is the dispersing effect that a tracer would have if the fluid was stagnant and secondly there is the effect caused by the diffusion between the streamlines, which attenuates the local concentration differences. The hydrodynamic dispersion for an incompressible fluid is usually described by the dispersion equation [23]

$$\frac{\partial C}{\partial t} = \nabla \cdot (\boldsymbol{D}\nabla C) - \boldsymbol{U}\nabla C \tag{1}$$

where $\boldsymbol{D}$ is the hydrodynamic dispersion tensor and $\boldsymbol{U}$ is the vector containing the linear velocities. For axial flow, the hydrodynamic dispersion tensor is reduced to the axial dispersion coefficient, D_x. In the chromatographic field the term equivalent plate height (H) is often used to describe the hydrodynamic dispersion. The equivalent plate height is related to the axial dispersion coefficient according to [10]

$$H_{\mathrm{hyd}} = \frac{2D_x t}{L_{\mathrm{c}}} = \frac{2D_x}{U} \tag{2}$$

where L_{c} is the column length and t the residence time.

In chromatographic applications both the convective and diffusive mechanisms usually contribute to the hydrodynamic dispersion, which is commonly described by models according to [10,24,25]

$$D_x = \frac{\lambda d_{\mathrm{p}} U}{1 + C_1(D_{\mathrm{m}}/d_{\mathrm{p}}U)} + \gamma D_{\mathrm{m}} \tag{3}$$

where C_1, λ and γ are experimentally determined coefficients, and D_{m} is the molecular diffusion coefficient. The hydrodynamic dispersion is often characterized by the Peclet number describing the ratio of the convective velocity to the diffusive velocity [23]

$$Pe = \frac{l_{\mathrm{c}} U}{D_{\mathrm{m}}} \tag{4}$$

where l_{c} is a characteristic length of the system and is highly dependent on the structure of the porous medium. The mechanism of hydrodynamic dispersion is dependent on the flow region. At very low Peclet numbers molecular diffusion is dominant, while at high Peclet numbers convective dispersion is dominant. The ratio of the hydrodynamic dispersion and the molecular diffusion coefficients is commonly correlated to the Peclet number. The following correlation for axial hydrodynamic dispersion has been suggested [23]:

$$\frac{D_x}{D_{\mathrm{m}}} = a\left(\frac{l_{\mathrm{c}}U}{D_{\mathrm{m}}}\right)^b, \quad \text{where } a \approx 0.5 \text{ and } 1 < b < 1.2 \tag{5}$$

At low Peclet numbers, b is close to 1.2. As b approaches 1 (Pe>300) the effect of the transverse molecular diffusion becomes negligible. Eq. (5) is valid for Peclet numbers between 5 and 10 000 [23,26]. The present study is restricted to high Peclet numbers.

For pure convective dispersion, i.e. at high Peclet numbers, the correlation length of a porous media may be described by [10]

$$l_{\mathrm{c}} = \omega d_{\mathrm{p}} \tag{6}$$

where ω is close to unity for an unconsolidated particulate medium [10,23]. A consolidated granular medium is characterized by a larger hydrodynamic dispersion than an unconsolidated medium, which may be interpreted as an increase in correlation length [9] and an increase in ω.

The ratio of the longitudinal dispersion coefficient to the transverse dispersion coefficient is commonly between 5 and 7 [23,26] in a porous medium. However, with Knox et al. [2] and Eon [3] found that the radial dispersion in a chromatographic column was approximately 25 times smaller than the axial dispersion at Peclet numbers in the range of 300. The radial dispersion is of little importance when predicting the performance of wide chromatographic columns.

In the present study the propagation of a concentration front was followed experimentally. The velocity profile as

well as the axial hydrodynamic dispersion coefficient was evaluated. The results were compared with computer simulations using a previously developed control-volume method [15,16,27].

3. Materials and methods

3.1. Experimental set-up

The experimental set-up is shown in Fig. 1. The column used was a BP113 column (Amersham Pharmacia Biotech, Sweden) with an inner diameter of 0.113 m. The distributors consisted of a support plate on which a coarse net, covered with a fine-meshed polyester net, was mounted. The mobile phase was fed through the centre of the support plate and the coarse net served as a spacer, ensuring an even distribution of the liquid. Sets of concentric electrodes were mounted at three axial positions inside the column to make dispersion measurements possible. Each set of electrodes consisted of four concentric electrodes made of stainless steel (wire diameter=1 mm) mounted at the following radial positions: 0.156*R*, 0.407*R*, 0.634*R* and 0.873*R*. The fifth electrode was painted on the column wall (Electrolube, Silver conductive paint) in order to be able to make measurements in the nearest proximity of the wall. The electrodes were partially shielded by an insulating lacquer in order to keep the output voltage at the same level for a given tracer concentration. The inner electrode was unshielded, and at the column wall approximately 25% of the electrode was unshielded. The active parts of the electrodes are shown in Fig. 1. Electrodes were also placed before the inlet and after the outlet of the column. The electrodes were connected to a conductivity meter [28] and a scanning switch, which was controlled by a PC using a Labmaster board (Tecmar). The scanning switch was specially built to fulfil the requirements set by the Labmaster board and the conductivity meter. The measurements were a succession of readings at each electrode level. Two radially adjacent electrodes were activated at a time. Each measurement result was an average of 500 discrete signals, which were obtained at a frequency of 1 kHz. The linearity of the conductivity measurements was excellent.

Mariotte bottles were used instead of pumps to obtain a pulse-free flow. The mass flow rate and the pressure drop were continuously recorded. The temperature was measured at the outlet of the column using a thermocouple (type K).

3.1.1. Stationary phase

Non-porous spherical glass beads were used to study the hydrodynamic dispersion in a rigid column, and a highly compressible, dextran-based chromatographic medium (Sephadex G-75, Pharmacia Biotech, Sweden) was used to study the flow and dispersion under compression. The highly compressible medium was chosen in order to obtain clear and distinct effects of the compression that could be used to verify the proposed model. The glass beads had a mean diameter of 177 μm and the size distribution (σ/d_p) was 0.19. The glass beads were dry-packed by pouring small portions of the beads into the column and then tamping them down. The Sephadex G-75 gel, with a mean diameter of 144 μm and a size distribution (σ/d_p) of 0.34, was packed by pouring a slurry consisting of three volumes of sedimented packing material and one volume of supernatant into the column. The particles were then allowed to pack at a constant flow rate ($U_0=0.8\times10^{-4}$ m^3/m^2 s) until the desired packing pressure was reached (8 kPa). When the gel had settled, the adaptor was lowered to the surface of the gel and was then fixed at that position. After the column was packed the direction of flow was reversed.

The height of the column packed with glass beads was 0.238 m, and the electrodes were situated at x=0.014, 0.110, and 0.217 m and the height of the Sephadex gel column was 0.313 m with the electrodes at x=0.084, 0.191 and 0.287 m.

The interstitial void fraction was calculated from the flow rate per unit area and the linear velocity ($\varepsilon=U_0/U$). The linear velocity was evaluated using the electrodes placed

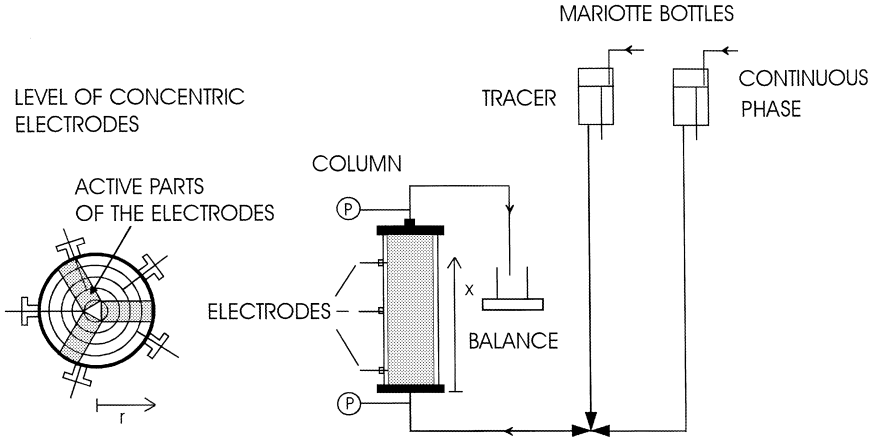

Fig. 1. Experimental set-up.

at the inlet and outlet. Corrections were made for the volume occupied by tubing and distributors. The same tracers were used as in the experiments described below. The inter-granular void fraction in the column containing glass beads was 0.368 and the average inter-granular void fraction of the Sephadex column was 0.237.

3.1.2. Mobile phase

The mobile phase was a NaCl solution, 0.018 g/l. In the glass bead column either NaCl (0.025 g/l), giving low Peclet numbers, or dextran sulphate (MW=500 000, 0.14 g/l), giving high Peclet numbers, was used as tracer and in the Sephadex column only dextran sulphate was used. The molecular diffusion coefficient of dilute NaCl in water at 25°C is 1.54×10^{-9} m^2/s [29] and the molecular diffusion coefficient of dextran sulphate was estimated to be 1.4×10^{-11} m^2/s, using diffusion data for dextran [30]. Temperature and viscosity corrections were performed using the Stoke–Einstein correlation stating that $D_m\,\mu/T$ is constant for a given solute [31]. According to the manufacturer's specifications for Sephadex G-75, the fraction range, expressed in MW for dextrans, is 1×10^3–5×10^4. By comparing the retention time for dextran sulphate and silica beads 70 nm in diameter, it was confirmed that dextran sulphate did not interact with the stationary phase. To obtain a constant flow rate the viscosities of the solutions were equalized ($\mu=1.16\times10^{-3}$ Pa s at 25°C) by adding methylcellulose, approximately 0.2 g/l, to the pure NaCl-solution. Both the dextran sulphate and the methylcellulose were purified by gel filtration (Sephadex G-75). Only the first, unretained fraction was used. The solutions were de-aerated under vacuum for 30–60 min. The experiments were performed at room temperature.

3.2. Experimental procedure

All experiments were performed at a steadystate, i.e. at constant flow rate and at constant temperature. A concentration step was introduced and the propagation of the concentration front was detected by the conductivity electrodes.

3.2.1. Calculations

Twelve local breakthrough curves were obtained in each experimental run. The hydrodynamic dispersion and the linear velocities were calculated by evaluating the variance, σ_t^2, and the mean time, $\bar{t}$, for each time–concentration curve. Since the measurements were performed inside the column, there was no need to make corrections for the dispersion caused by the distributors or other external sources, such as tubing. The axial linear velocity between two electrodes was calculated from [32]

$$U = \frac{\Delta x}{\bar{t}_2 - \bar{t}_1} \tag{7}$$

where Δx is the axial distance between the electrodes. The hydrodynamic dispersion coefficient was obtained from [32]

$$\frac{\sigma_{t_2}^2 - \sigma_{t_1}^2}{\Delta t^2} = 2\left(\frac{D_x}{U\,\Delta x}\right) \tag{8}$$

where $\sigma_{t_1}^2$ and $\sigma_{t_2}^2$ are the variances at two axial positions and Δt is the corresponding time interval which was calculated from the mean values of the concentration steps.

The influence of the radial dispersion was investigated by computer simulations [16]. It was confirmed that the radial dispersion is of little importance when predicting the performance of the column under investigation.

4. Results and discussion

The quality of the packing was investigated by comparing the experimental recordings with the analytical one-dimensional solution of the dispersion Eq. (1) given by [32]

$$\frac{C(x,t)}{C_0} = \frac{1}{2}\left[\operatorname{erfc}\left(\frac{x-Ut}{2\sqrt{D_x t}}\right) + \exp\left(\frac{Ux}{D_x}\right)\operatorname{erfc}\left(\frac{x+Ut}{2\sqrt{D_x t}}\right)\right] \tag{9}$$

Macroscopic packing anomalies are identified by deviations in the third moment, the skewness. The concentration fronts measured by the inner electrodes (Figs. 2b–d and 3) agreed well with the fronts calculated analytically using Eq. (9). This indicates that the packing of the column was macroscopically homogenous, and that the electrodes did not introduce any significant packing anomalies. Close to the column wall the concentration fronts for both packings showed a slightly anomalous shape as seen in Figs. 2a and 3. This is an indication of packing irregularities caused by the proximity of the wall.

4.1. Hydrodynamic dispersion

The hydrodynamic dispersion was evaluated between the first and third set of electrodes at four radial positions (see Fig. 1). In each experimental run the local dispersion coefficients (D_x) were normalized against the mean dispersion coefficient in the core ($\bar{D}_x$). The variation in the axial dispersion across a segment of the column packed with glass beads is shown in Fig. 4a. The dispersion in the wall region (r>0.049 m) is typically two to four times higher than in the core (r<0.049 m) and does not depend on flow rate. The same dispersion pattern, i.e. a core region exhibiting a small variation in dispersion and a wall region with anomalous dispersion has been previously observed in chromatographic columns [2,3,6].

The variation in the axial dispersion across a segment of the column packed with Sephadex gel is shown in Fig. 4b. A broader wall region (r>0.036 m) was found compared to the glass bead packing. The variation in axial dispersion is, however, significantly smaller than for the glass bead

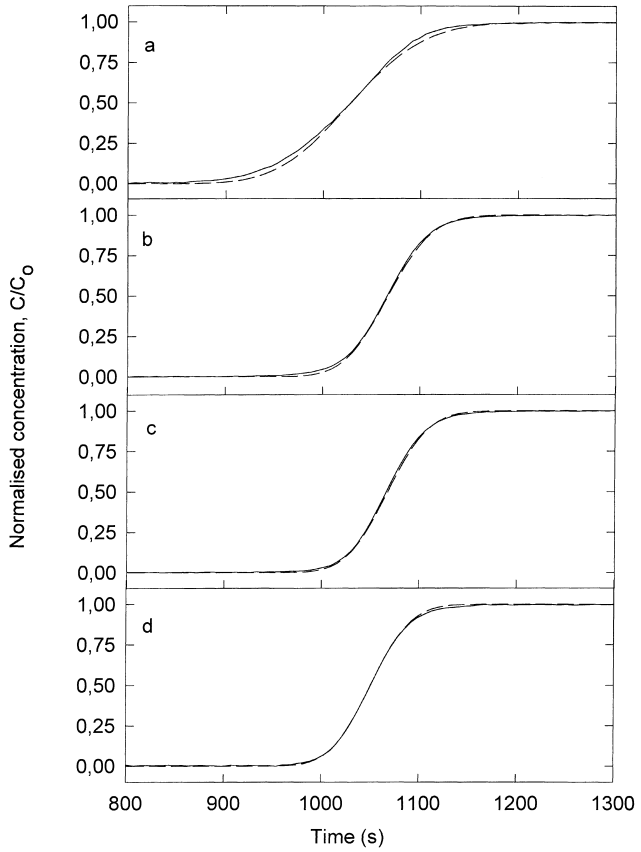

Fig. 2. Local normalized concentration fronts in a column packed with rigid spherical glass beads measured at x=0.217 m. The radial positions were according to: (a) r=0.0565–0.049 m; (b) r=0.049–0.036 m; (c) r=0.036–0.023 m; (d) r=0.023–0.009 m. (—) Experimental values; (- -)best fit curve according to Eq. (9). The column length was 0.238 m, the column radius 0.0565 m and the void fraction 0.368. NaCl was used as tracer.

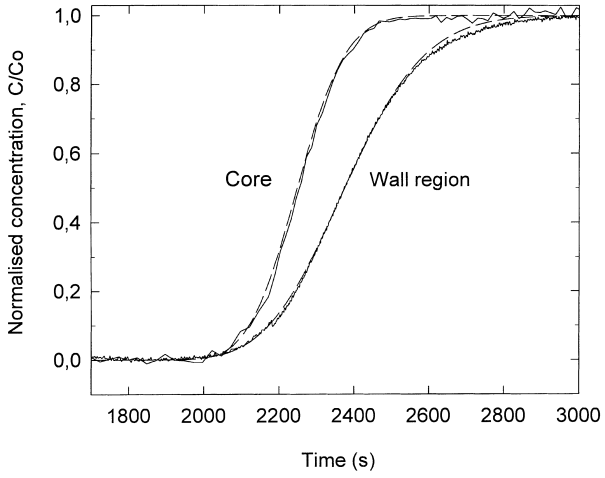

Fig. 3. Local normalized concentration fronts in a column packed with Sephadex G-75 measured at x=0.287 m. The radial positions were r=0.023–0.009 m (core) and r=0.0565–0.049 m (wall region). (—) Experimental values; (- -) best fit curve according to Eq. (9). The column length was 0.313 m, and the column radius 0.0565 m. The void fraction was 0.237, the flow rate 0.26 ml/s, the viscosity 1.002×10^{-3} Pa s and the pressure drop 2.2 kPa. The tracer was dextran sulphate.

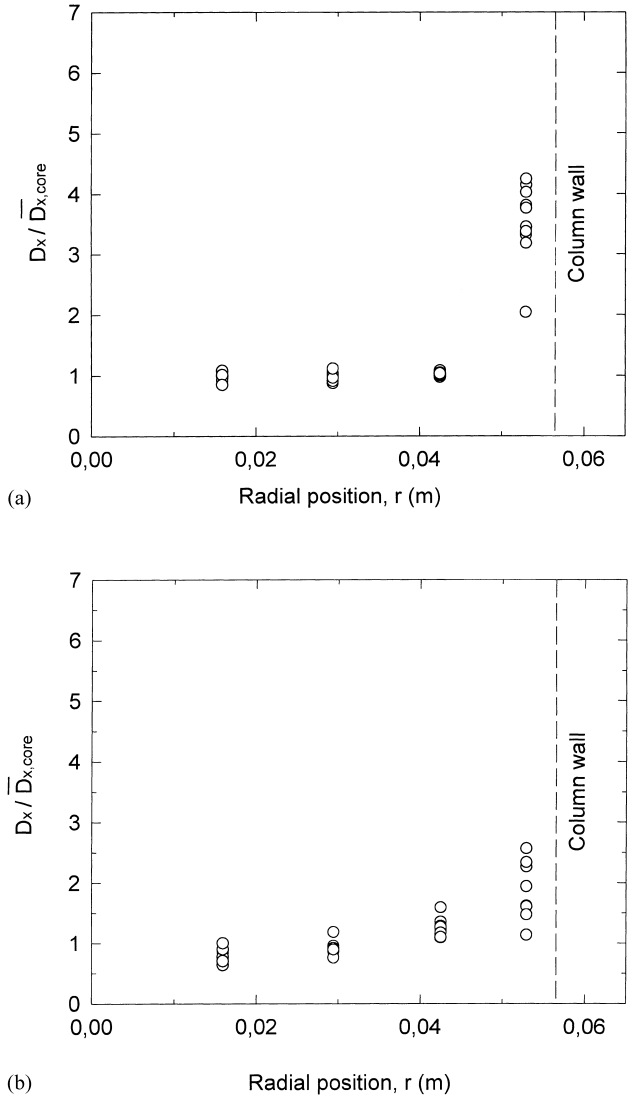

Fig. 4. Dispersion variation across a segment of a column. The dispersion measurements were made between the first and last electrode level using dextran sulphate as a tracer. The dispersion coefficients were normalized to the mean value obtained from the inner positions (the core) in each experiment. (a) Dispersion measurements in a column packed with glass beads. The electrodes were placed at x=0.014 and 0.217 m. The superficial velocity was between 1.4×10^{-5} and 29×10^{-5} m^3/m^2 s. (b) Dispersion variation across a segment of a column packed with Sephadex gel. The electrodes were placed at x=0.084 and 0.287 m. The superficial velocity was between 2.4×10^{-5} and 3.5×10^{-5} m^3/m^2 s.

packing, indicating that the compression of the gel evens out the packing anomalies close to the wall.

The axial hydrodynamic dispersion coefficients were evaluated in the core of the chromatographic bed. The core was characterized by small radial and axial flow variations. An average value of the three inner measurement positions in the rigid packing, and of the two inner positions in the Sephadex packing, were used. The increase in the axial linear velocity due to compression was less than 15% between the two electrode levels used in the evaluation and a mean value could thus be used with negligible loss in the overall accuracy of

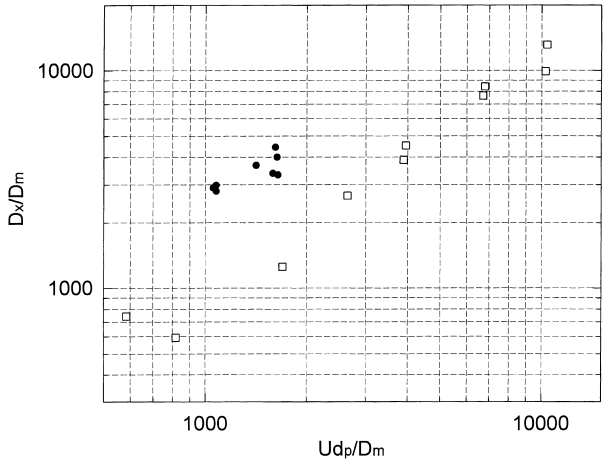

Fig. 5. Hydrodynamic dispersion vs. Peclet number. Tracer: dextran sulphate. (□) Glass beads, x=0.014–0.217 m; (●) Sephadex gel, x=0.084–0.191 m.

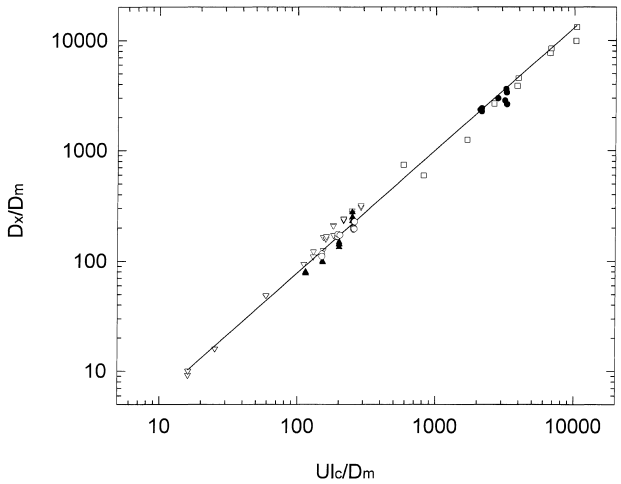

Fig. 6. Hydrodynamic dispersion vs. Peclet number. (▽) Glass beads, ε=0.368, $l_c=d_p$, tracer: NaCl; (▲) glass beads, ε=0.369, $l_c=d_p$, tracer: NaCl [33]; (○) glass beads, ε=0.361, $l_c=d_p$, tracer: NaCl [33]; (□) glass beads, ε=0.368, $l_c=d_p$, tracer: dextran sulphate; (●) Sephadex gel, ε=0.237, $l_c=2d_p$, tracer: dextran sulphate; (—) correlation according to Eq. (10).

the calculated dispersion coefficients. Fig. 5 shows the experimental, axial hydrodynamic dispersion coefficients, normalized against the molecular diffusion coefficient, plotted vs. the Peclet number. According to the results shown in Fig. 5, the dispersion in the compressed bed was a factor of two higher than expected for the rigid bed under the same experimental conditions. According to our previous study [33] on hydrodynamic dispersion in columns containing glass beads, the difference in size distribution between the glass beads and the Sephadex gel is too small to be responsible for the increased hydrodynamic dispersion in the compacted column. It thus appears that the increased dispersion is due to geometrical changes in the interparticle void space. These results are thus in qualitative agreement with previous findings, showing that the consolidation of a granular medium increases the correlation length [9]. The structural parameter ω in Eq. (6) describes the ratio between the actual correlation length and the correlation length in an ideal unconsolidated particulate packing. For the glass bead packing ω is approximately one and for the Sephadex packing ω is approximately two.

The experimental results for the glass bead packing agree well with data in the literature [26,34]. The dispersion data for both types of packing could be correlated to the Peclet number according to Eq. (10)

$$\frac{D_x}{D_m} = 0.47\left(\frac{l_c U}{D_m}\right)^{1.1} \tag{10}$$

assuming a characteristic length of $l_c=d_p$ for the glass bead packing and $l_c=2d_p$ for the compressible Sephadex packing (Fig. 6).

4.2. Linear velocities

The variations in the axial linear velocity across a segment of the column for the glass bead packing are shown in Fig. 7a. The velocity profile is flat except in the vicinity of the wall, where the linear velocity was on average about 10% higher than in the core.

Previous experimental investigations of velocity variations in rigid chromatographic columns packed with incompressible particles show similar results, i.e. an even distribution in the core region and a wall region exhibiting different properties. Knox et al. [2], Eon [3] and Baur et al. [7] found that the velocity increased in the vicinity of the wall, while Farkas et al. [6] found a velocity maximum at a distance of approximately 0.6R and Baur et al. [7] found that the velocity had an optimum close to the wall, when using a radially compressed column. Thus, the effect of the wall seems to be very much dependent on the chromatographic system being investigated.

The velocity profile in the column packed with Sephadex gel (Fig. 7b) was rather different from that found for the rigid packing. In this case the linear velocity close to the wall was lower than or very nearly the same as the linear velocity in the core. According to Fig. 7b the lowest velocity near the wall relative to that at the core is found at low flow rates. In order to find an explanation, we used our previously developed computer code [15,16,27] to simulate the velocity field. A pure elastic deformation of the chromatographic bed [15] was assumed. The parameters used in the flow-compression calculations and the initial conditions are summarized in Table 1. Typical variations of the linear velocity, relative to the centre of the column, at low flow rates are shown in Fig. 8a. It can be seen that the velocity near the wall is smaller than the velocity at the centre close to the inlet, and greater near the wall close to the outlet. The velocity variations are due to the interplay between the stress originating from the flow and the stress originating from the column terminals and the influence of the wall fric-

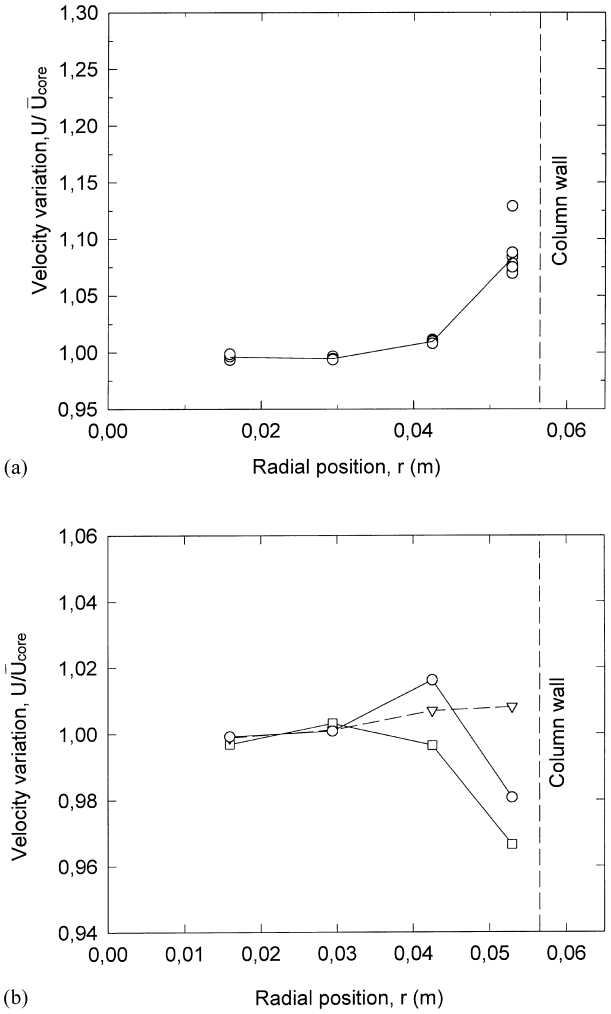

Fig. 7. Linear velocity variations across a segment of a column. The measurements were made between the first and third electrode levels and dextran sulphate was used as a tracer. (a) Velocity variations in a column packed with glass beads between x=0.014 and 0.217 m. (b) Velocity variation for different flow rates in a column packed with Sephadex gel between x=0.084 and 0.287 m. (□) q=0.26 ml/s; (○) q=0.34 ml/s; (▽) q=0.42 ml/s. The flow rates are recalculated to correspond to the reference viscosity $\mu=1.002\times10^{-3}$ Pa s.

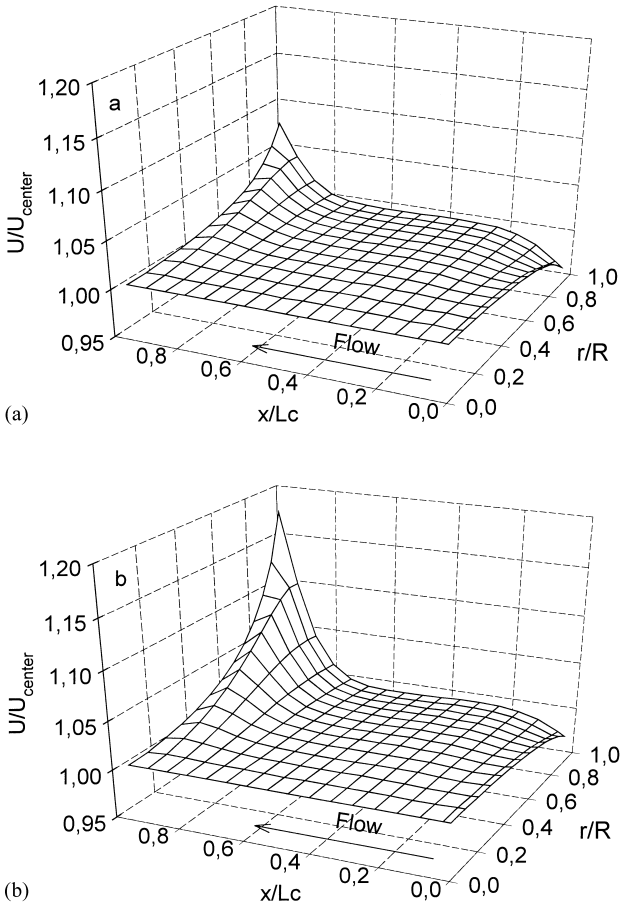

Fig. 8. Predicted variation in the axial linear velocity (U) relative to the values at the centre line (U_{centre}) in a column packed with Sephadex G-75. The parameters describing the flow and compression are given in Table 1. (a) q=0.26 ml/s and ΔP=2.2 kPa, (b) q=0.42 ml/s and ΔP=4.2 kPa.

tion, which opposes the compaction [27]. As the linear velocity increases, a larger fluid stress is taken up by the matrix and the column compacts to a larger extent at the outlet and a different flow field, which is less influenced by the column terminals, is obtained (Fig. 8b). Thus, the computer simulations shown in Fig. 8a and b provide an explanation of the observed change in velocity profile (Fig. 7b) with increased flow rate. The experimental local velocity profiles and the corresponding simulated values are shown in Fig. 9. To make more accurate predictions, non-uniformities in the chromatographic bed that are not due to the compression must be quantified and also included in the model. It should also be emphasized that the use of different packing techniques and different chromatographic media may give rise to initial conditions being different from those found to be appropriate in this study (Table 1), which in turn will lead to different velocity profiles.

Table 1
Parameters of importance in the simulation of the velocity profile[a]

Column dimensions	Packing characteristics	Mechanical properties of the gel [15]	Initial condition [27]	Fluid properties
R=0.0565 m, $L_{c=}$0.313 m	$d_{ps}=178\times10^{-6}$ m, ε_{mean}=0.237, $k=[d_{ps}^2/180][\varepsilon^3/(1-\varepsilon^2)]$	$E=5.63\times10^4\varepsilon^2-8.39\times10^4\varepsilon+2.77\times10^4$ Pa, ν=0.27, $\mu_{f=}$0.16	A pure mechanical load on an initially homogeneous, relaxed bed.	μ=0.001 Pa s, ρ=1000 kg/m^3

[a] R=column radius, L_c=column length, d_{ps}=surface-based particle diameter, ε_{mean}=average void fraction, E=Young's modulus, ν=Poisson ratio, μ_f=wall friction coefficient, μ=viscosity, ρ=fluid density.

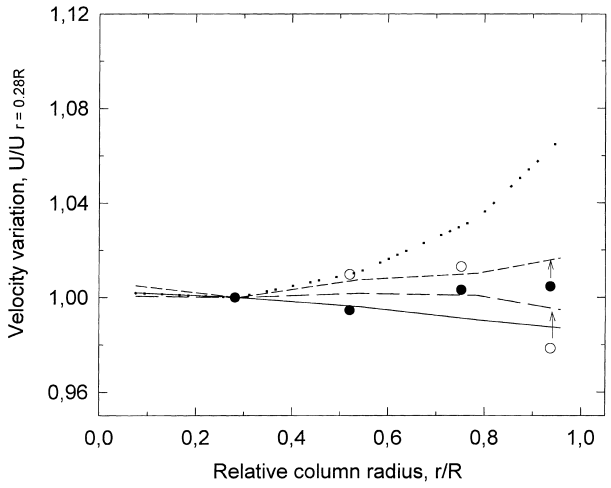

Fig. 9. Experimental and predicted axial velocity variations across a column at different axial positions. The local values of U are normalized with $U_{r=0.28R}$, which corresponds to the experimental point closest to the centre of the column. (—) x=0–0.084 m, predicted; (— —) x=0.088–0.19 m, predicted; (○) x=0.088–0.19, experimental; (- -) x=0.19–0.29 m, predicted; (●) x=0.19–0.29 m, experimental; (···) x=0.29–0.313, predicted. The arrows mark the corresponding computed and experimental values. The column was packed with Sephadex gel and the parameters describing the flow and compression are given in Table 1. The pressure drop was 2.2 kPa and the flow rate was 0.26 ml/s. The experimental velocities are recalculated to correspond to the reference viscosity $\mu=1.002\times10^{-3}$ Pa s.

The experimentally determined variation in the linear velocity along the column packed with the Sephadex gel and predicted values are shown in Fig. 10. The shape of the profiles reflects the changes in structure of the gel along the column. The experimental and predicted profiles agreed fairly well. The predicted flow rates were 16% lower than the measured, but considering the complexity of the model and the fact that no parameter fitting has been carried out, we find this discrepancy acceptable.

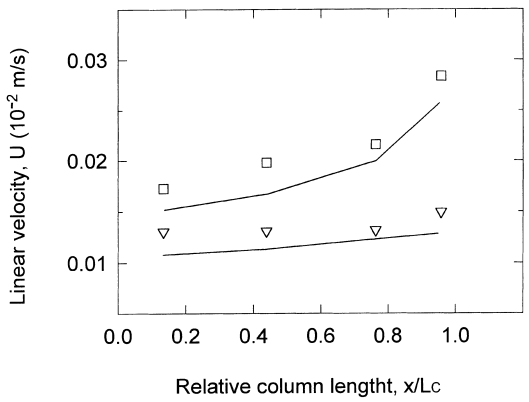

Fig. 10. Experimental (□,▽) and computed (—) axial velocity variations at the centre of a chromatographic column packed with Sephadex G-75; (▽) q=0.26 ml/s, ΔP=2.2 kPa; (□) q=0.42 ml/s, ΔP=4.2 kPa. The parameters describing the flow and compression are shown in Table 1. The experimental velocities are recalculated to correspond to the reference viscosity $\mu=1.002\times10^{-3}$ Pa s.

The spread of a concentration front along a chromatographic column is determined by the local hydrodynamic dispersion, the local variation in the linear velocity and the mass transport in the radial direction, i.e. radial convective transport and radial hydrodynamic dispersion. The total increase in band broadening due to the predicted velocity variations in the column packed with Sephadex gel (Fig. 8) was investigated by computer simulations by solving Eq. (1) numerically [16]. The local axial dispersion coefficients were predicted from Eq. (10). The elution profiles were compared with elution profiles neglecting the axial velocity variations across the column. It was found that the predicted velocity profiles, as given in Fig. 8, contributed less than 2% to the overall band broadening.

5. Conclusions

The flow and dispersion in a compressible, chromatographic bed have been experimentally characterized. The results were compared with those found in a chromatographic column packed with glass beads of approximately the same size and size distribution. The results were also compared with values predicted by the numerical simulations using a two-dimensional model describing the flow and compression of a chromatographic bed [15,16,27].

The experimental part of this work shows that both columns could be described by a homogeneous core, characterized by plug flow and high column efficiency, and a wall region, characterized by fairly large velocity variations and increased hydrodynamic dispersion. The velocity variations and the anomalies in the hydrodynamic dispersion in the vicinity of the wall were smaller in the column packed with the compressible chromatographic gel than in the column packed with glass beads. The results found for the rigid column are in accordance with measurements performed by others [2,3] and can most probably be explained by irregularities in the packing close to the wall. According to the measurements performed in this study the compression of non-rigid particles partly evens out these irregularities. It was also found that the local hydrodynamic dispersion in the core of the compressed bed was approximately twice the hydrodynamic dispersion expected for homogenous rigid packing comprized of glass beads. For the compressible chromatographic bed it was shown, by computer simulations, that the axial velocity profile developed across the column, neglecting the wall effects, contributed to a very small extent to the overall band broadening. Thus, two significant effects of compression influencing the overall band broadening were found. The first was a decrease in band broadening due to smaller velocity and dispersion variations in the vicinity of the column wall. Secondly, there was an increase in the local hydrodynamic dispersion, presumably due to a different pore geometry.

Computed axial velocity variations were compared with experimental variations and were found to agree qualitatively.

6. List of symbols

C	tracer concentration (g/l)
C_0	initial tracer concentration (g/l)
d_p	particle diameter (μm)
$\boldsymbol{D}$	hydrodynamic dispersion tensor (m^2/s)
D_m	molecular diffusion coefficient (m^2/s)
D_x	coefficient of axial hydrodynamic dispersion (m^2/s)
$\bar{D}_x$	mean axial dispersion coefficient in the core (m^2/s)
H	equivalent plate height (m)
k	coefficient of permeability (m^2)
l_c	correlation length (m)
L_c	column length (m)
Pe	Peclet number (Ul_c/D_m) (dimensionless)
r	radial distance from column centre (m)
R	column radius (m)
t	time (s)
U	linear velocity in axial direction (m/s)
U_0	superficial velocity (m^3/m^2 s)
x	axial distance (m)

Greek letters

γ	experimentally determined coefficient (dimensionless)
ε	inter-granular void fraction (dimensionless)
λ	experimentally determined coefficient (dimensionless)
μ	viscosity (Pa s)
μ_f	wall friction (dimensionless)
σ	standard deviation
σ_t	standard deviation (time) (s)
σ_t^2	variance (time) (s^2)
ω	structural parameter (dimensionless)

Acknowledgements

The authors wish to acknowledge financial support for this study provided by the Swedish Board for Technical and Industrial Development and are indebted to Amersham Pharmacia Biotech AB, Sweden for supplying chromatographic media and the column.

References

[1] G.K. Sofer, L.E. Nyström, Process Chromatography, A Practical Guide, Academic Press, London, 1989.
[2] J.H. Knox, G.R. Laird, P.A. Raven, J. Chromatogr. 22 (1976) 129–145.
[3] C. Eon, J. Chromatogr. 149 (1978) 29–42.
[4] T. Yun, G. Guiochon, J. Chromatogr. A 672 (1994) 1–10.
[5] J.H. Knox, J.F. Patcher, Anal. Chem. 41 (1969) 1599–1605.
[6] T. Farkas, J.Q. Chambers, G. Guiochon, J. Chromatogr. A 679 (1994) 231–245.
[7] J.E. Baur, E.W. Kristensen, R.M. Wightman, Anal. Chem. 60 (1988) 2334–2338.
[8] N.S. Mitchell, L. Hagel, E.J. Fernandez, J. Chromatogr. A 779 (1997) 73–89.
[9] E. Charlaix, J.P. Hulin, T.J. Plona, Phys. Fluids 30 (1987) 1690–1698.
[10] J.C. Giddings, Dynamics of Chromatography, Part 1. Principles and Theory, Marcel Dekker, New York, 1965.
[11] R.M. Nicoud, M. Perrut, Chromatogr. Sci. 61 (1993) 47–77.
[12] A.M. Wilhelm, J.P. Riba, G. Muratet, A. Peyrouset, R. Prechner, J. Chromatogr. 363 (1986) 113–123.
[13] B. Porsch, J. Chromatogr. A 658 (1994) 179–194.
[14] G. Guiochon, M. Sarker, J. Chromatogr. A 704 (1995) 269–277.
[15] K.C.E. Östergren, C. Trägårdh, G.G. Enstad, J. Mosby, AIChE J. 44 (1998) 2–12.
[16] K. Östergren, C. Trägårdh, Numer. Heat Transfer A 32 (1997) 247–265.
[17] R.F. Benenati, C.B. Brosilow, AIChE J. 8 (1962) 359–361.
[18] M.K. Jostrua, A. Emnéus, P. Tibbling, in: H. Peeters (Ed.), Protides of the Biological Fluids, Elsevier, Amsterdam, Vol. 15, 1967, pp. 575–579.
[19] J.-C. Janson, P. Hedman, in: A. Fiechter (Ed.), Advances in Biochemical Engineering, Vol. 25: Chromatography, Springer, Heidelberg, 1982, pp. 43–99.
[20] F.H. Verhoff, J.J. Furjanic, Ind. Eng. Chem. Process. Des. Dev. 22 (1983) 192–198.
[21] P.A. Davies, B.J. Bellhouse, Chem. Eng. Sci. 44 (1989) 452–455.
[22] F.M. Tiller, W.-M. Lu, AIChE J. 18 (1972) 569–572.
[23] J. Bear, Dynamics of fluids in porous media, Elsevier, New York, 1972.
[24] C.L. DeLigny, J. Chromatogr. 49 (1970) 393–401.
[25] M. Magnico, M. Martin, J. Chromatogr. 517 (1990) 31–49.
[26] R.A. Greenkorn, Flow Phenomena in Porous Media. Fundamentals and Applications in Petroleum, Water and Food Production, Marcel Dekker, New York, 1983.
[27] K. Östergren, C. Trägårdh, Chem. Eng. J. 72 (1999) 153–161.
[28] M. Ahmond, Electronics 15 (1977) 132.
[29] R.C. Weast (Ed.), Handbook of Chemistry and Physics, 55th Edition, CRC Press, Cleveland, 1974.
[30] K. Granat, J. Colloid Sci. 13 (1958) 308–328.
[31] P.W. Atkins, Physical Chemistry, Oxford University Press, Oxford, 1979, pp. 833–835.
[32] O. Levenspiel, Chemical Reaction Engineering, Wiley, New York, 1972, 253–315.
[33] K. Östergren, C. Trägårdh, in: D.L. Pyle (Ed.), Separations for Biotechnology, Vol. 2, Elsevier, London, 1990, pp. 632–640.
[34] N.-W. Han, J. Bhakta, R.G. Carbonell, AIChE J. 31 (1985) 277–287.